# Fractal Dimension in the Directed Landscape in the Temporal Direction


Lingfu Zhang

Princeton University
Department of Mathematics


Apr 29, 2022
Probability and Statistical Physics Seminar
The University of Chicago
arXiv:2204.01674
Joint work with Shirshendu Ganguly

# Random Planar Geometry

# General FPP Model

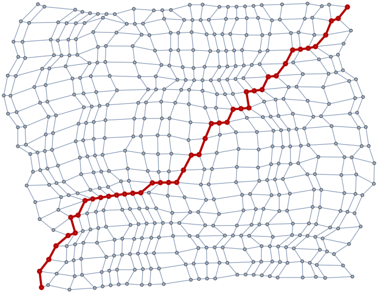

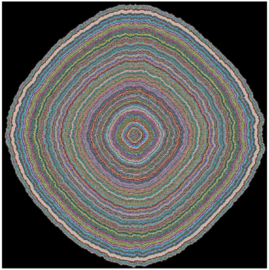

Figure from Dauvergne and Virág, 2021.

First Passage Percolation: a canonical random metric.

- Lattice $\mathbb{Z}^2$.
- For each edge, assign i.i.d. (non-negative) weight.
- Distance between any two vertices: smallest total weight.
- Geodesic: path with minimum weight.

First order: limit shape
Next order: believed to be in the KPZ universality class.

# Exactly-Solvable Setting

A classical example:
directed Last Passage Percolation (LPP) with exponential weights.

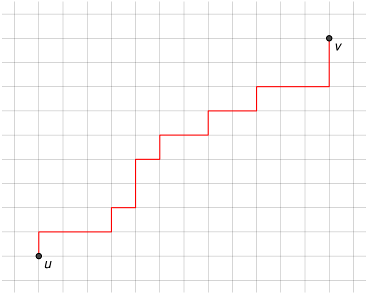


- $\xi(v) \sim \text{Exp}(1)$, i.i.d. $\forall v \in \mathbb{Z}^2$
- Passage time: $L_{u,v} := \max_\gamma \sum_{w \in \gamma} \xi(w)$, over all directed paths.
- Geodesic: path with **maximum** weight.

Exactly-solvable using algebraic combinatorics, representation theory, or queueing.

# Exactly-Solvable Setting

A classical example:
directed Last Passage Percolation (LPP) with exponential weights.

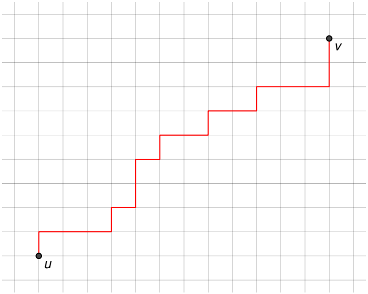


- $L_{(0,0),(n,n)} \sim 4n$ (Rost, 1981).
- $2^{-4/3}n^{-1/3}(L_{(0,0),(n,n)} - 4n)$ converges to the GUE Tracy-Widom distribution, and geodesic has $n^{2/3}$ fluctuation (Johansson, 2000).
- Point to line profile (Borodin and Ferrari, 2008)

$$2^{-4/3}n^{-1/3}\left(L_{(0,0),(n-x(2n)^{2/3},n+x(2n)^{2/3})} - 4n\right) \Rightarrow \mathcal{A}_2(x) - x^2.$$

# Exactly-Solvable Setting

A classical example:
directed Last Passage Percolation (LPP) with exponential weights.

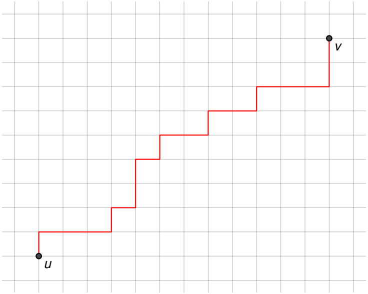


Some other exactly-solvable settings:

- LPP with geometric weights.
- LPP through a Poisson field.
- LPP through a sequence of Brownian motions.
- Uniform random permutations.

Limit: the Directed Landscape; believed to be the limit of general FPP.

# Scaling Limit

The directed landscape is a random 'directed metric' on $\mathbb{R}^2$, constructed in Dauvergne, Ortmann, and Virág, 2018.
For any $(x, r)$, $(y, t)$ with $r < t$, $\mathcal{L}(x, r; y, t)$ is the passage time.

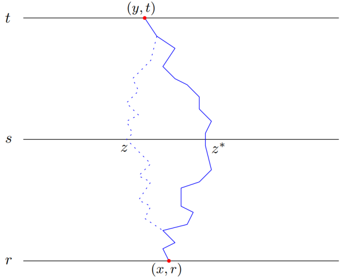


Figure from Dauvergne, Ortmann, and Virág, 2018.

Anti-triangle inequality

$$\mathcal{L}(x, r; y, t) \geq \mathcal{L}(x, r; z, s) + \mathcal{L}(z, s; y, t).$$

Composition:

$$\mathcal{L}(x, r; y, t) = \max_{z} \mathcal{L}(x, r; z, s) + \mathcal{L}(z, s; y, t).$$

# Scaling Limit

The directed landscape is a random 'directed metric' on $\mathbb{R}^2$, constructed in Dauvergne, Ortmann, and Virág, 2018.
For any $(x, r)$, $(y, t)$ with $r < t$, $\mathcal{L}(x, r; y, t)$ is the passage time.

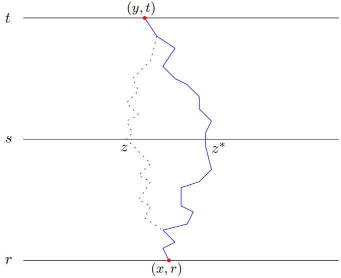


Figure from Dauvergne, Ortmann, and Virág, 2018.

Path weight: for a continuous function $\pi : [r, t] \to \mathbb{R}$ with $\pi(r) = x$ and $\pi(t) = y$,

$$\|\pi\|_{\mathcal{L}} = \inf_{r=t_0<t_1<\ldots<t_k=t} \sum_{i=1}^{k} \mathcal{L}(\pi(t_{i-1}), t_{i-1}; \pi(t_i), t_i).$$

Geodesic: maximum weight $\|\pi\|_{\mathcal{L}} = \mathcal{L}(x, r; y, t)$.

# Convergence from Exponential LPP

Roughly,

$$2^{-4/3}n^{-1/3}\left(L_{(nr+2^{5/3}n^{2/3}x,nr),(nt+2^{5/3}n^{2/3}y,nt)}-4n(t-r)-2^{8/3}n^{2/3}(y-x)\right)$$
$$\to \mathcal{L}(x,r;y,t).$$

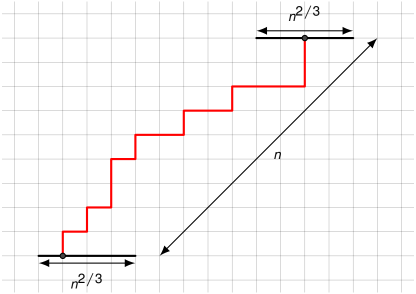


Jointly for the geodesics: convergence after the transformation

$$(a,b)\mapsto(2^{-5/3}n^{-2/3}(b-a),n^{-1}b).$$

(Dauvergne and Virág, 2021, also for convergence of other exactly-solvable models.)

# Some Basic Symmetries

Reflection by spatial/temporal axis:

$$(x, r; y, t) \mapsto \mathcal{L}(y, -t; x, -r), \quad (x, r; y, t) \mapsto \mathcal{L}(-x, r, -y, t)$$

Shift:

$$(x, r; y, t) \mapsto \mathcal{L}(x + z, r + s; y + z, t + s)$$

# Some Basic Symmetries

Reflection by spatial/temporal axis:

$$(x, r; y, t) \mapsto \mathcal{L}(y, -t; x, -r), \quad (x, r; y, t) \mapsto \mathcal{L}(-x, r, -y, t)$$

Shift:

$$(x, r; y, t) \mapsto \mathcal{L}(x + z, r + s; y + z, t + s)$$

Affine shift:

$$(x, r; y, t) \mapsto \mathcal{L}(x+cr, r; y+ct, t)+(t-r)^{-1}((x-y+c(r-t))^2-(x-y)^2)$$

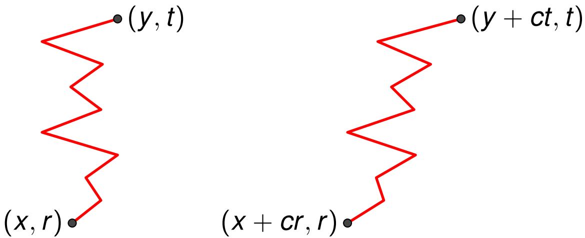

## Some Basic Symmetries

Reflection by spatial/temporal axis:

$$(x, r; y, t) \mapsto \mathcal{L}(y, -t; x, -r), \quad (x, r; y, t) \mapsto \mathcal{L}(-x, r, -y, t)$$

Shift:

$$(x, r; y, t) \mapsto \mathcal{L}(x + z, r + s; y + z, t + s)$$

Affine shift:

$$(x, r; y, t) \mapsto \mathcal{L}(x+cr, r; y+ct, t)+(t-r)^{-1}((x-y+c(r-t))^2-(x-y)^2)$$

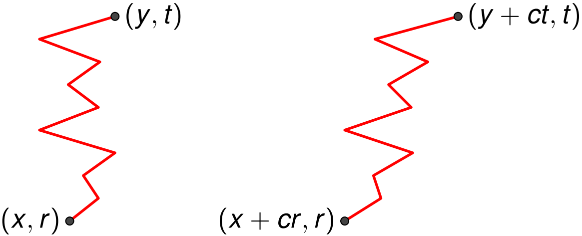


Scaling:

$$(x, r; y, t) \mapsto w\mathcal{L}(w^{-2}x, w^{-3}r; w^{-2}y, w^{-3}t)$$

Source of fractal behaviours.

# Difference Profile

# Quadrangle Inequality and Coalescence

For each $x$, $\mathcal{L}(x, 0; x + \cdot, 1)$ is a parabolic Airy$_2$ process ($\mathcal{A}_2(y) - y^2$).
What is the coupling structure for different $x$?

Such 'directed metric' behaves differently from a normal metric: geodesics tend to coalesce

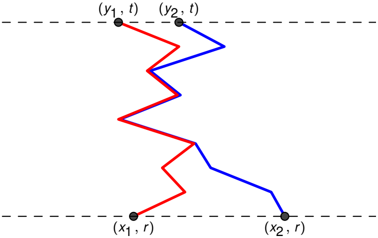


Coalesce if $|x_1 - x_2|$ or $|y_1 - y_2|$ is small enough.

Quadrangle inequality:
for $x_1 < x_2$, $y_1 < y_2$, and $r < t$,

$$\mathcal{L}(x_1, r; y_1, t) + \mathcal{L}(x_2, r; y_2, t) \geq \mathcal{L}(x_1, r; y_2, t) + \mathcal{L}(x_2, r; y_1, t).$$

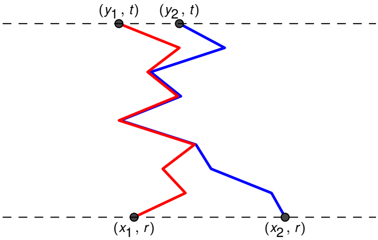

Quadrangle inequality:
for $x_1 < x_2$, $y_1 < y_2$, and $r < t$,

$$\mathcal{L}(x_1, r; y_1, t) + \mathcal{L}(x_2, r; y_2, t) \geq \mathcal{L}(x_1, r; y_2, t) + \mathcal{L}(x_2, r; y_1, t).$$

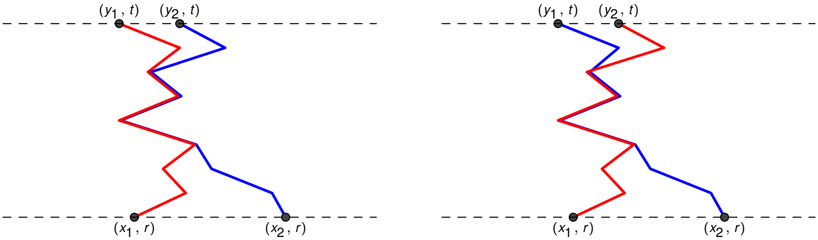


Equality holds if and only if the geodesics from $(x_1, r)$ to $(y_1, r)$ and from $(x_2, r)$ to $(y_2, r)$ coalesce.

# Difference Profile: Almost Everywhere Locally Constant

Take two points (e.g. $(-1,0)$ and $(1,0)$), consider the difference profile

$$\mathcal{D}(x,r) = \mathcal{L}(1,0;x,r) - \mathcal{L}(-1,0;x,r).$$

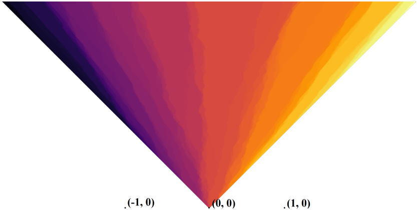


Simulation by Milind Hegde.

It is almost everywhere locally constant:

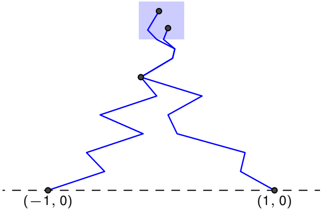

Take two points (e.g. $(-1, 0)$ and $(1, 0)$), consider the difference profile

$$\mathcal{D}(x, r) = \mathcal{L}(1, 0; x, r) - \mathcal{L}(-1, 0; x, r).$$

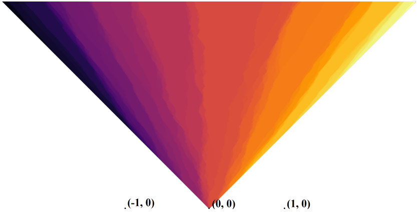


Simulation by Milind Hegde.

Non-constancy: disjoint geodesics
(Bates, Ganguly, and Hammond, 2019)

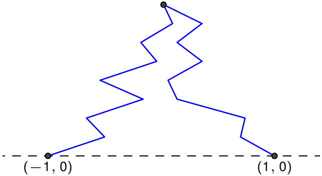

# Non-constancy Set of the Difference Profile: Spatial Direction

In Basu, Ganguly, and Hammond, 2019, such difference profile in the spatial direction (i.e. $\mathcal{D}(\cdot, 1)$) was studied.

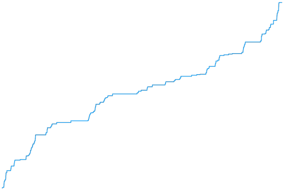

Simulation by Milind Hegde.

Monotone: $\mathcal{D}(x_1, 1) \leq \mathcal{D}(x_2, 1)$, since (by the quadrangle inequality)

$$\mathcal{L}(1, 0; x_2, 1) + \mathcal{L}(-1, 0; x_1, 1) \geq \mathcal{L}(1, 0; x_1, 1) + \mathcal{L}(-1, 0; x_2, 1).$$

Can interpret $\mathcal{D}(\cdot, 1)$ as the CDF of a measure on $\mathbb{R}$.

This measure is supported inside the non-constancy set in $\mathbb{R} \times \{1\}$.

Next: Hausdorff dimension of the spatial direction set.

**Hausdorff dimension:**
For any $d \geq 0$ and metric space $X$, the $d$-dimensional Hausdorff measure of $X$ is defined as

$$\lim_{\delta \searrow 0} \inf \Big\{ \sum_i \mathrm{diam}(U_i)^d : \{U_i\} \text{ is a countable cover of } X \text{ with } 0 < \mathrm{diam}(U_i) < \delta \Big\}.$$

The Hausdorff dimension of $X$ is

$$\inf\{d > 0 : \text{ the } d\text{-dimensional Hausdorff measure of } X \text{ is zero } \}.$$

# Non-constancy Set of the Difference Profile: Spatial Direction Fractal

**Hausdorff dimension:**
For any $d \geq 0$ and metric space $X$, the $d$-dimensional Hausdorff measure of $X$ is defined as

$$\lim_{\delta \searrow 0} \inf \Big\{ \sum_i \mathrm{diam}(U_i)^d : \{U_i\} \text{ is a countable cover of } X \text{ with } 0 < \mathrm{diam}(U_i) < \delta \Big\}.$$

The Hausdorff dimension of $X$ is

$$\inf\{d > 0 : \text{ the } d\text{-dimensional Hausdorff measure of } X \text{ is zero } \}.$$

**Lower bound:**

If there is a non-zero measure supported inside $X \subset \mathbb{R}$, and its CDF is $\alpha$-Hölder, then the Hausdorff dimension of $X$ is at least $\alpha$.

**For spatial non-constancy set:**
Both $\mathcal{L}(1, 0; \cdot, 1)$ and $\mathcal{L}(-1, 0; \cdot, 1)$ are parabolic Airy$_2$, thus locally Brownian
$\Rightarrow \mathcal{D}(\cdot, 1)$ is $(1/2 - \delta)$-Hölder.

**Hausdorff dimension:**
For any $d \geq 0$ and metric space $X$, the $d$-dimensional Hausdorff measure of $X$ is defined as

$$\lim_{\delta \searrow 0} \inf \Big\{ \sum_i \mathrm{diam}(U_i)^d : \{U_i\} \text{ is a countable cover of } X \\ \text{with } 0 < \mathrm{diam}(U_i) < \delta \Big\}.$$

The Hausdorff dimension of $X$ is

$$\inf\{d > 0 : \text{ the } d\text{-dimensional Hausdorff measure of } X \text{ is zero } \}.$$

**Upper bound:**

Cover $X$ by $\epsilon^{-1/2}$ sets, each with diameter $< \epsilon$.

**For spatial non-constancy set:**
Given any interval, divide it into $\epsilon^{-1}$ small intervals, each with length $\sim \epsilon$; $\mathcal{D}(\cdot, 1)$ is non-constant on each with probability $< \epsilon^{1/2}$.
This is reduced to the disjointness of the geodesics from $(-1, 0)$ to $(x, 1)$ and from $(1, 0)$ to $(x + \epsilon, 1)$.
(Upper bound of probability available from Hammond, 2019)

Consider $\mathcal{D}(0, \cdot)$:

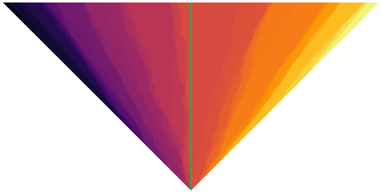

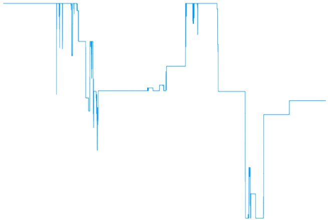

Simulations by Milind Hegde.

**Lower bound:** $\mathcal{L}$ is $(1/3 - \epsilon)$-Hölder in the temporal direction, so the non-constancy set in $\{0\} \times \mathbb{R}_+$ has Hausdorff dimension $\geq 1/3$.

**Upper bound:** $\mathcal{D}(0, \cdot)$ being non-constant in $[t, t + \epsilon]$ can be 'reduced' to the disjointness of the geodesics from $(-1, 0)$ to $(-\epsilon^{2/3}, t)$ and from $(1, 0)$ to $(\epsilon^{2/3}, t)$.
The probability is $\sim \epsilon^{1/3}$ by Hammond, 2019.
$\Rightarrow$ the non-constancy set in $\{0\} \times \mathbb{R}_+$ has Hausdorff dimension $\leq 2/3$.

# Temporal Direction: Hausdorff Dimension

Consider $\mathcal{D}(0, \cdot)$:

Simulations by Milind Hegde.

Why they do not match in the temporal direction?
Heuristic explanation: no monotonicity and cancellations.

Consider a random walk in a $2/3$-dimensional fractal set: will be $(1/3 - \epsilon)$-Hölder.

# Temporal Direction: Hausdorff Dimension

Consider $\mathcal{D}(0,\cdot)$:

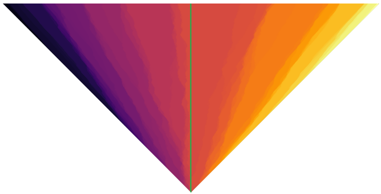
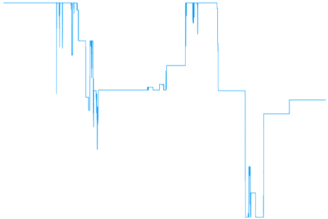

Simulations by Milind Hegde.

Why they do not match in the temporal direction?
Heuristic explanation: no monotonicity and cancellations.

Consider a random walk in a $2/3$-dimensional fractal set: will be $(1/3-\epsilon)$-Hölder.

**Theorem**

*The non-constancy set of $\mathcal{D}(0,\cdot)$ has Hausdorff dimension $2/3$.*
*The non-constancy set of $\mathcal{D}$ has Hausdorff dimension $5/3$.*

# Decomposition and Geodesic Local Time

# Level Set Decomposition

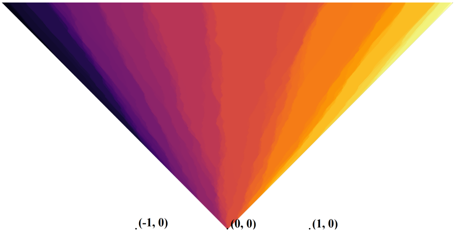


Simulation by Milind Hegde.

Consider

$$\vartheta_\ell(t) = \sup\{x \in \mathbb{R} : \mathcal{D}(x,t) \le \ell\}.$$

Non-constancy set is the union of level sets.

**Idea:**

- Construct local time for $\vartheta_\ell$.
- Consider the measure given by the average (over $\ell$) of the local times.
- Prove Hölder property and non-degeneracy.

# An Analog of Brownian Local Time

Brownian local time:

$$\lim_{w \to 0} (2w)^{-1} \int_0^h \mathbb{1}[-w \leq \mathcal{B}(t) \leq w] dt.$$

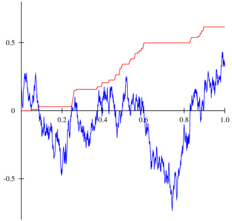


Simulation from Kostrykin, Potthoff, and Schrader, 2012

# An Analog of Brownian Local Time

Brownian local time:

$$\lim_{w\to 0}(2w)^{-1}\int_0^h \mathbb{1}[-w \le \mathcal{B}(t) \le w]dt.$$

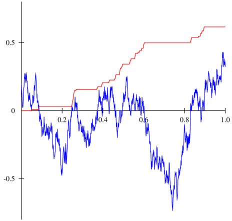


Simulation from Kostrykin, Potthoff, and Schrader, 2012

Like the Brownian local time, we define the local time of $\vartheta_\ell$:

$$\kappa_\ell([g,h]) = \lim_{w\to 0}(2w)^{-1}\int_g^h \mathbb{1}[-w \le \vartheta_\ell(t) \le w]dt.$$

Consider the measure $\kappa = \int \kappa_\ell d\ell$. It is also supported inside the non-constancy set! $\Rightarrow$ **aim at showing that it is $2/3$-Hölder**

# An Analog of Brownian Local Time

Brownian local time:

$$\lim_{w \to 0} (2w)^{-1} \int_0^h \mathbb{1}[-w \le \mathcal{B}(t) \le w] dt.$$

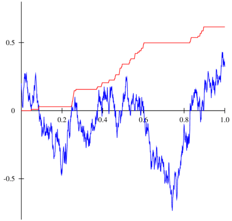


Simulation from Kostrykin, Potthoff, and Schrader, 2012

Like the Brownian local time, we define the local time of $\vartheta_\ell$:

$$\kappa_\ell([g, h]) = \lim_{w \to 0} (2w)^{-1} \int_g^h \mathbb{1}[-w \le \vartheta_\ell(t) \le w] dt.$$

Consider the measure $\kappa = \int \kappa_\ell d\ell$. It is also supported inside the non-constancy set! $\Rightarrow$ **aim at showing that it is $2/3$-Hölder**

- Roughly $\kappa([g, g+\epsilon]) < \epsilon^{1/3} \sup_\ell \kappa_\ell([g, g+\epsilon])$.

# Level Set Decomposition: Comparison to Competition Interface

$\vartheta_\ell$ can be understood as a competition interface (two narrow wedge).

- Also consider the competition interface from Brownian initial data:

$$\mathcal{L}^L(x,t) = \sup_{y\leq 0} \mathcal{L}(y,0;x,t) + \mathcal{B}(y),$$

$$\mathcal{L}^R(x,t) = \sup_{y\geq 0} \mathcal{L}(y,0;x,t) + \mathcal{B}(y),$$

$$\vartheta^{\mathcal{B}}(t) = \sup\{x \in \mathbb{R} : \mathcal{L}^L(x,t) - \mathcal{L}^R(x,t) \leq 0\}.$$

# Level Set Decomposition: Comparison to Competition Interface

$\vartheta_\ell$ can be understood as a competition interface (two narrow wedge).

- Also consider the competition interface from Brownian initial data:

$$\mathcal{L}^L(x,t) = \sup_{y \le 0} \mathcal{L}(y,0;x,t) + \mathcal{B}(y),$$
$$\mathcal{L}^R(x,t) = \sup_{y \ge 0} \mathcal{L}(y,0;x,t) + \mathcal{B}(y),$$

$$\vartheta^{\mathcal{B}}(t) = \sup\{x \in \mathbb{R} : \mathcal{L}^L(x,t) - \mathcal{L}^R(x,t) \le 0\}.$$

**Key property:** $\vartheta^{\mathcal{B}} \overset{d}{=} \pi_{(0,0)}$

(This is the semi-infinite geodesic, also constructed in e.g. Busani, Seppäläinen, and Sorensen, 2022; Rahman and Virág, 2021).

- Duality known for exponential LPP.
  (See e.g. Ferrari, Martin, and Pimentel, 2009. Limit transition also done in Rahman and Virág, 2021)

# Level Set Decomposition: Comparison to Competition Interface

Make $\mathcal{B}$ spiky, and assume coalescence of geodesics.

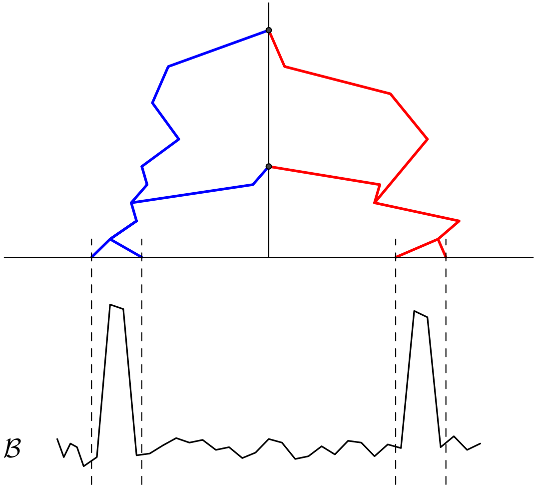


In an interval, $\vartheta^{\mathcal{B}}$ is $\vartheta_\ell$ for some random $\ell$.

# Geodesic Local Time

Local time of $\vartheta^{\mathcal{B}}$ (equivalently, geodesic local time):

$$\kappa^{\mathcal{B}}([g,h]) = \lim_{w\to 0}(2w)^{-1}\int_g^h \mathbb{1}[\vartheta^{\mathcal{B}}(t) \in [-w,w]]dt.$$

This is also '$\kappa_\ell$ with random $\ell$'.
Can show that:

$\kappa^{\mathcal{B}}([g,g+\epsilon])$ is at most in the order of $\epsilon^{1/3}$ with exponential tail.

(By multi-scale analysis of the semi-infinite geodesic, from Sarkar, Sly, and Zhang, 2021)
$\Rightarrow \sup_\ell \kappa_\ell([g,g+\epsilon])$ is at most in the order of $\epsilon^{1/3}$
$\Rightarrow \kappa([g,g+\epsilon])$ is at most in the order of $\epsilon^{2/3}$; i.e. $\kappa$ is $2/3$-Hölder
$\Rightarrow$ Non-constancy set of $\mathcal{D}(0,\cdot)$ has Hausdorff dimension $\geq 2/3$.

Local time of $\vartheta^{\mathcal{B}}$ (equivalently, geodesic local time):

$$\kappa^{\mathcal{B}}([g,h]) = \lim_{w\to 0}(2w)^{-1}\int_g^h \mathbb{1}[\vartheta^{\mathcal{B}}(t)\in[-w,w]]dt.$$

This is also '$\kappa_\ell$ with random $\ell$'.
Can show that:

$\kappa^{\mathcal{B}}([g,g+\epsilon])$ is at most in the order of $\epsilon^{1/3}$ with exponential tail.

(By multi-scale analysis of the semi-infinite geodesic, from Sarkar, Sly, and Zhang, 2021)
$\Rightarrow \sup_\ell \kappa_\ell([g,g+\epsilon])$ is at most in the order of $\epsilon^{1/3}$
$\Rightarrow \kappa([g,g+\epsilon])$ is at most in the order of $\epsilon^{2/3}$; i.e. $\kappa$ is $2/3$-Hölder
$\Rightarrow$ Non-constancy set of $\mathcal{D}(0,\cdot)$ has Hausdorff dimension $\geq 2/3$.

- An implication for the semi-infinite geodesic:

**Theorem**

*The set* $\{t>0:\pi_{(0,0)}(t)=0\}$ *has Hausdorff dimension* $1/3$.

Thank you!

Basu, R., Ganguly, S., & Hammond, A. (2019). **Fractal geometry of Airy$_2$ processes coupled via the Airy sheet** [arXiv preprint arXiv:1904.01717].

Bates, E., Ganguly, S., & Hammond, A. (2019). **Hausdorff dimensions for shared endpoints of disjoint geodesics in the directed landscape** [arXiv preprint arXiv:1912.04164].

Borodin, A., & Ferrari, P. L. (2008). Large time asymptotics of growth models on space-like paths I: PushASEP. **Electron. J. Probab.**, **13**, 1380–1418.

Busani, O., Seppäläinen, T., & Sorensen, E. (2022). **The stationary horizon and semi-infinite geodesics in the directed landscape** [arXiv preprint arXiv:2203.13242].

Dauvergne, D., Ortmann, J., & Virág, B. (2018). The directed landscape [to appear]. **Acta Math.**

Dauvergne, D., & Virág, B. (2021). **The scaling limit of the longest increasing subsequence** [arXiv preprint arXiv:2104.08210].

Ferrari, P. A., Martin, J. B., & Pimentel, L. P. R. (2009). A phase transition for competition interfaces. **Ann. Appl. Probab.**, **19**(1), 281–317.

Hammond, A. (2019). Exponents governing the rarity of disjoint polymers in brownian last passage percolation [to appear]. **Proc. Lond. Math. Soc.**

Johansson, K. (2000). Shape fluctuations and random matrices. **Comm. Math. Phys.**, **209**(2), 437–476.

Kostrykin, V., Potthoff, J., & Schrader, R. (2012). Brownian motions on metric graphs. **Journal of mathematical physics**, **53**(9), 095206.

Rahman, M., & Virág, B. (2021). **Infinite geodesics, competition interfaces and the second class particle in the scaling limit** [arXiv preprint arXiv:2112.06849].

Rost, H. (1981). Non-equilibrium behaviour of a many particle process: Density profile and local equilibria. **Zeitschrift f. Warsch. Verw. Gebiete**, **58**(1), 41–53.

Sarkar, S., Sly, A., & Zhang, L. (2021). **Infinite order phase transition in the slow bond TASEP** [arXiv preprint, arXiv:2109.04563].